

AIAA 97-1482
Large Gliding Parachute
Experimental and Theoretical Approaches

Jean-Pierre Tribot,
Frédéric Chalot,
Marc Rapuc
Dassault Aviation, Saint-Cloud, F
Gilbert Durand
Centre National d'Etudes Spatiales, Toulouse, F

**14th AIAA Aerodynamic Decelerator
Systems Technology and Conference**
June 2-5, 1997/San Francisco, CA

Large Gliding Parachute, Experimental and Theoretical Approaches

J-P TRIBOT*, F. CHALOT*, M. RAPUC*, G. DURAND**

* DASSAULT AVIATION, Saint-Cloud, F

** EUROPEAN SPACE AGENCY/ CENTRE D'ETUDES SPATIALES, Toulouse, F

Abstract

The capability of gliding parachute to have a lift of drag ratio enough to reduce the landing site is best of interest to minimize the recovery cost of spacecraft like classical or advanced capsules.

In Europe, studies and demonstrator, sponsored by ESA/CNES, are in progress so as to assess the aerodynamic characteristics and to determine the behavior of this kind of complex configuration. This paper describes the strategy proposed by DASSAULT AVIATION. The baseline is to identify the main parameters governing the aerodynamic behavior. 3D numerical tools able to take into account a nonrigid body are improved and adapted to wind tunnel rebuilding. For wind tunnel, an aerodynamic balance designed for the gliding parachute tests is presented. Comparisons between numerical prediction and experimental data are discussed.

1. History

The last tendency related to the European space program are for a project less technically critical than HERMES spacecraft either for the development cost or for the life operation. To fulfill the requirements a new project is designed splitting the hypersonic reentry (cross range capability and flexibility in operation) and the landing phase (accurate landing).

This last technical point is a major point and needs about terminal and recover phases studies. The design criteria for such recover system must include the following items :

- * **mass**
- * **landing accuracy**
- * **sensibility to atmosphere conditions (wind, turbulence,...)**
- * **reliability and safety**

The recovery system might have a lift over drag ratio enough in order to reduce the landing site and consequently minimize the recovery team on zone. In addition, an horizontal and vertical speeds as low as possible is required to be able to generate a soft landing (flare phase) so as to minimize the load during the touch down for crew members.

A recovery system by means of « gliding parachute » could be a solution.

Since 1993, in EUROPE, recovery system studies, sponsored by ESA/CNES through different space programs (Assured Crew Return Vehicle , Non Winged Return Vehicle, Crew Transport Vehicle, Parafoil Technology Demonstrator [*DASA as prime contractor*] and MSTP « Prediction Tools for Classical Capsule » [*AEROSPATIALE as prime contractor*]), were done or are in progress for the last programs PTD and MSTP « capsule ».

DASSAULT AVIATION is involved in these activities and brings its expertise in the experimental and theoretical aerodynamic fields.

2. Wind Tunnel Experiment

By comparisons with flight tests, wind tunnel tests are interesting due to the fact that they provide a lot of detailed informations in terms of general observations during the inflation and tests, in terms of aerodynamic coefficients, loads in suspension line, gliding parachute angle of attack and pressure coefficient itself. Also, the wind tunnel tests should provide some tests clearly identify for numerical tools validation. The wind tunnel test could be best of interest to verify the rigging angle pre-selected for the configuration. By means of special device the angle of attack (i.e rigging angle in flight) of the gliding parachute could be modify so as to assess the general characteristics of the airfoil and to determine the limit in flight operation.

A list of relevant European wind tunnel available for « gliding parachute tests » allowed to show that ONERA S1 Modane wind tunnel as the larger facility available in Europe. The stilling chamber (ϕ 24 m) is used as test chamber and the freestream condition is up to 24 m/s. This wind tunnel is able to test a gliding parachute up to 80 m² representative of a large model and to provide a Reynolds number closed to the flight.

Some improvements within the stilling chamber were done in order to install the aerodynamic balance under the wind tunnel floor. This original design allows to modify the general configuration of the wind tunnel without removing the gliding parachute aerodynamic balance. Parachute wind tunnel tests could start again without delay.

A complete study related to the aerodynamic balance was done by Dassault Aviation. In addition with the determination of the classical aerodynamic coefficient, this balance has a specific

device allowing to modify the angle of attack of the parachute during tests.

A large parachute (71m²) tested in S1ma was designed with a CLARK « Y » airfoil. This model is a downscaling of a flight model (scale ratio \approx 1/2). Different angle of attack with different symmetrical trailing edge defection were investigated.

3. Numerical simulation

Due to the complex aerodynamic phenomena which occurred around a gliding parachute configuration, one have to proceed step by step in order to assess the wing characteristics and to isolate the main parameters governing the general behavior. First, a simplified method is applied in order to quantify different assumptions related to the gliding parachute geometry, afterwards a Navier-Stokes calculation is performed so as to identify the viscous effect and then a Navier-Stokes calculation with structure coupling is computed to exhibit the material - flowfield interaction.

3.1 Singularities method

Aerodynamic derivatives that contributes to stability and guidance are generated by interference of deformation of geometry and perturbation in the flows, DASSAULT AVIATION designed four geometries derivatives from the reference one. The reference geometry is based on the CLARK « Y » airfoil without cell inflated in spanwise direction and without trailing edge deflected. The derivatives are issued from the observations done during wind tunnel tests.

When the gliding parachute is completely inflated in the test chamber, we observe the following configuration :

- the trailing edge seems slightly deflected. This phenomena occurs when the dynamic pressure is not enough to insure a well inflation. In that case, the drag generated by the suspension line settled at the trailing edge and unloaded induced this deflection.

- the leading edge has a rounded part at the upper part of the air intake.
- due to the aerodynamic load located on the first 25% of the airfoil, the general airfoil shape seems to be a « banana » type.
- in spanwise direction, the geometry definition is driven by the cell inflation shape.

The geometrical derivatives (Figures 1-5) from the observations are summarized below :

1. *reference shape*
2. *reference + trailing edge deflected*
3. *2 + realistic trailing edge*
4. *3 + « banana » shape*
5. *4 + cells inflated*

Singularities method assuming that the flowfield attached is considered and the suspension lines contribution is not taken into account. The analysis of the numerical results shows that the deflection of the trailing edge (case 2) increases the lift coefficient - the rounded part of the leading edge (case 3) limits the flowfield acceleration and consequently generates a lower lift coefficient than the case 2 - the « banana » shape (case 4) gives the higher lift and drag coefficients then the case 5 being the most realistic geometry shows a lower lift coefficient than the case 4 (mainly induced by the spanwise shape generated by the cell inflation). Experimental data - numerical results comparisons exhibit a lift coefficient predicted by calculation higher about 50% for lift coefficient and 4% higher for lift over drag ratio. The present calculations do not take into account the viscous effect. In the rear part of the leeward side, the trailing edge deflected induces a separation of the flowfield. The preliminary results show a viscous effect non negligible and the initial prediction could be improved using a Navier-Stokes simulation. The effect of geometrical disturbances induced by the aerodynamic flowfield are non

negligible for the general behavior of the configuration. The preliminary results demonstrate the need to take into account the aero-structure coupling so as to refine the prediction.

3.2 3D Navier-Stokes calculation

The usage of unstructured grids have long time been motivated by the necessity to employ meshes made of the merely-necessary number of nodes (and sometimes less), in non-trivial geometries, and to permit simple local mesh daptation, in particular by element division. The following code has the possibility of treating any kind of element. Not only tetraedra, but also hexaedra, prisms, pyramids have been introduced. The solvers are able to deal with geometries discretized with any mixing of above kind of elements. The gliding parachute unstructured mesh (75 000 nodes) is generated by means of "EMAIL" DASSAULT AVIATION's software.

The DASSAULT AVIATION's Navier stokes code, called "VIRGINI", uses a finite element approach, the system of partial differential equations being written under weak formulation. The formulation implemented has a good stable characteristic and accuracy by means of using of Galerkin/least-squares (GLS) method. Although, the GLS is a stable method, oscillations may occur in the vicinity of strong gradients. A nonlinear discontinuity-capturing operator is added to the formulation. Convergence to steady state of the compressible Navier Stokes equations is achieved through an implicit iterative time-marching algorithm.

The code is based on a symmetric form of the equations written in terms of entropy variables.

Different turbulence model are available (K- ϵ , wall function, etc ...)

An aero-structure option exists within VIRGINI code

Full vectorized and parallel versions exist.

The VIRGINI code has been intensively used during the HERMES program for low and high speed configurations.

Related to the gliding parachute application, a turbulent calculation (wall function), using parallel option of the VIRGINI code has been performed on IPM SP2 16 processors.

The general configuration in wind tunnel is presented on figure 6. The wind tunnel configuration is different from those observed in flight where the payload insures the global equilibrium. In wind tunnel, the gliding parachute is hold at a fixed point and an equilibrium status (function of the lift over drag ratio) is found where the aerodynamic load is compensated by the floor resultant (pitching moment nul) for a given freestream condition.

4. Discussions

5. Conclusions

Experimental tests and numerical rebuilding of large gliding parachute in subsonic flow have been presented. Experimental activities included a study of a specific device able to modify the gliding parachute angle of attack as well as the description of the technic measurements used so as to assess the global aerodynamic coefficients and the geometrical definition of the parafoil during the tests.

In order to help the analysis of the experimental tests and contribute to the extrapolation ground-to-flight a computational fluid dynamic studies of the model tested in wind tunnel has allowed to identify the parameters governing the general feature of the configuration. Previously, a simplified method has been applied and shown the viscous effect and the geometrical definition effect by comparisons with experimental data.

The DASSAULT AVIATION's Navier-Stokes code has been adapted so as to take into account the non rigid body of the gliding parachute as well as the specific wind tunnel configuration.

The general features of the large gliding parachute in wind tunnel has been reproduced by the numerical code. Due to the possibility of limited test budgets and time constraints associated with the design of a recovery parachute systems, the numerical tools could be useful and must modelized the aerodynamic and structural behavior of the gliding parachute.

Some improvements should be best of interest so as to increase the level of modelization :

- porosity of the material
- suspension line contribution
- material properties

The strategy presented in this paper lead to progress step by step in order to isolate the main parameters governing the general behavior of the large gliding parachute in steady state. In the future, others aspects of the recovery phase should be to modelize like the configuration in turn and the flare before impact.

6. Acknowledgement

The authors wish to thank P. PERRIER (DA A) and J.F. RIVES (AERAZUR) for fruitful discussions. They also thank B. STOUFFLET and al for their contribution.

7. References

[ref(1)] : "A Comprehensive Finite Element Navier-Stokes Solver for Low and High Speed Aircraft Design", F. CHALOT, M. MALLET, M. RAVACHOL
AIAA Paper 94-0814, Reno, 1994

[ref(2)] : « HERMES, theoretical aerothermodynamic report on level 3" (private communication)

[ref(3)]: « Advanced Recovery Systems
Wind Tunnel Test Report »
R.H. Geiger and W.K. Wailes
NASA Contractor report 1777563

[ref(4)]: « Parachute Recovery Systems »
Design manual, T.W. Knacke
Para Publihsing, Santa Barbara, California

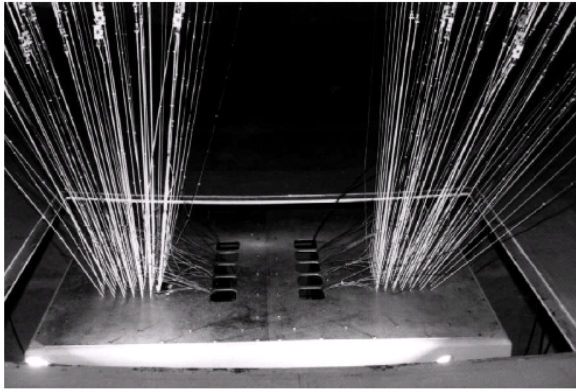


Figure 5. Perforated plate and rigging implementation

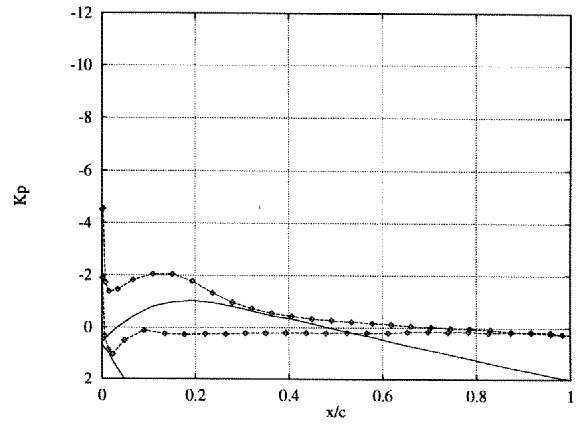


Figure 8. Reference shape (Shape #1)

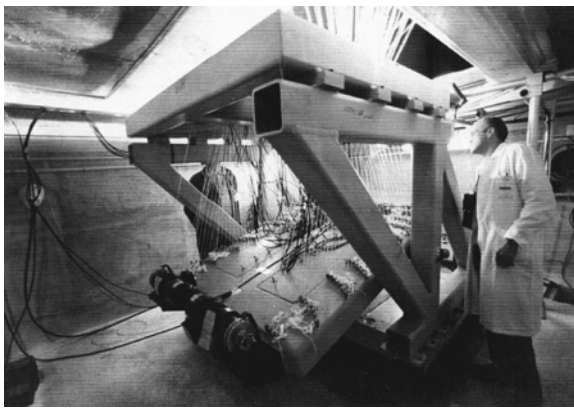


Figure 6. Balance room

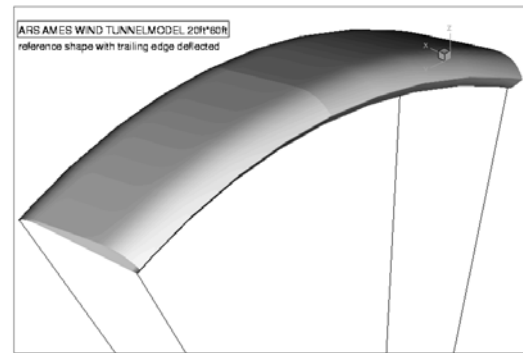


Figure 9. Reference shape with trailing edge deflection (Shape #2)

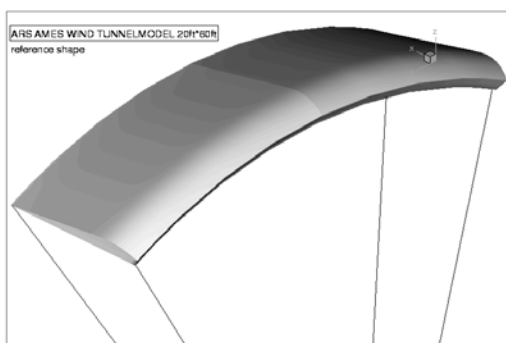


Figure 7. Reference shape (Shape #1)

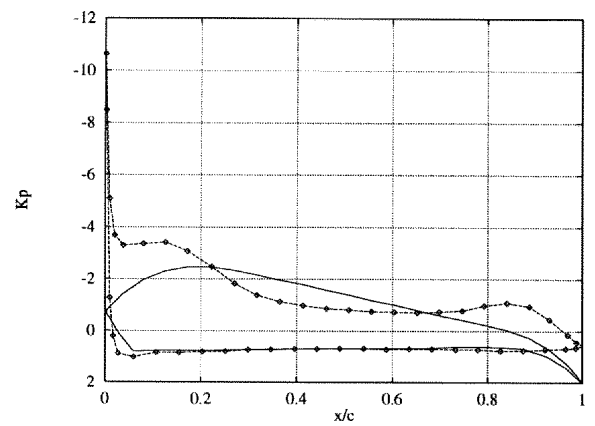


Figure 10. Reference shape with trailing edge deflection (Shape #2)

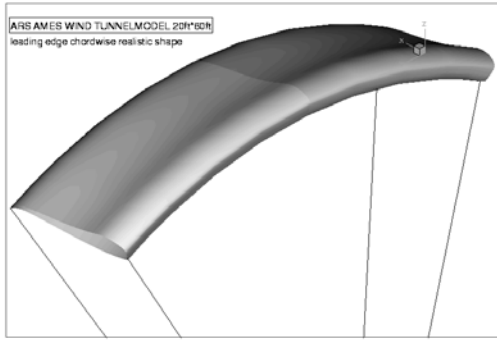


Figure 11. Shape #2 with rounded leading edge (Shape #3)

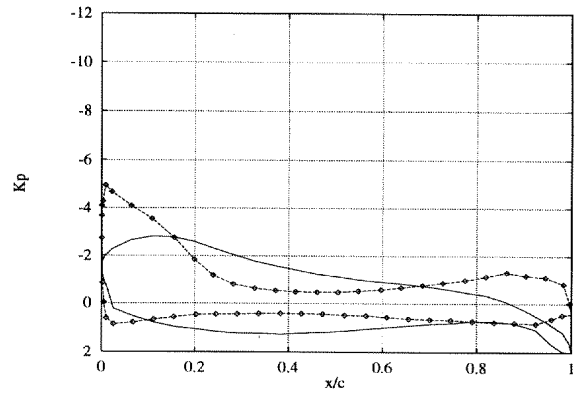


Figure 14. Shape #3 with camber (shape #4)

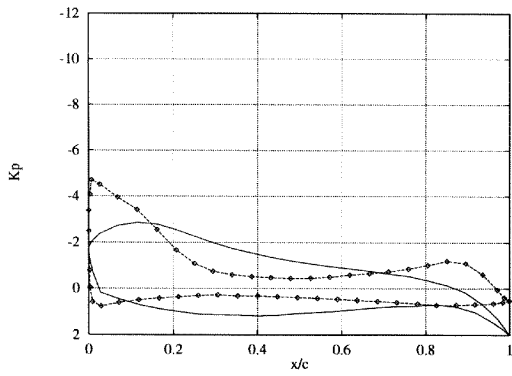


Figure 12. Shape #2 with rounded leading edge (Shape #3)

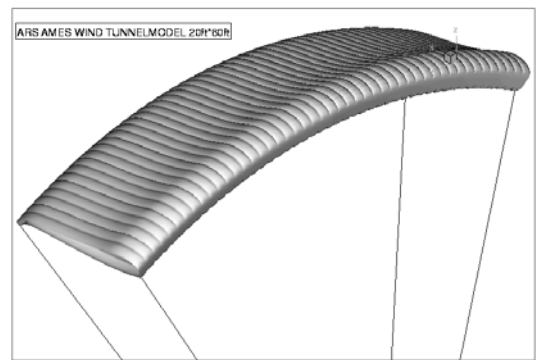


Figure 15. Shape #4 with inflated cells (Shape #5)

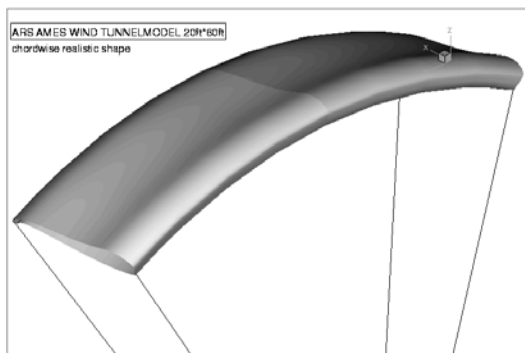


Figure 13. Shape #3 with camber (shape #4)

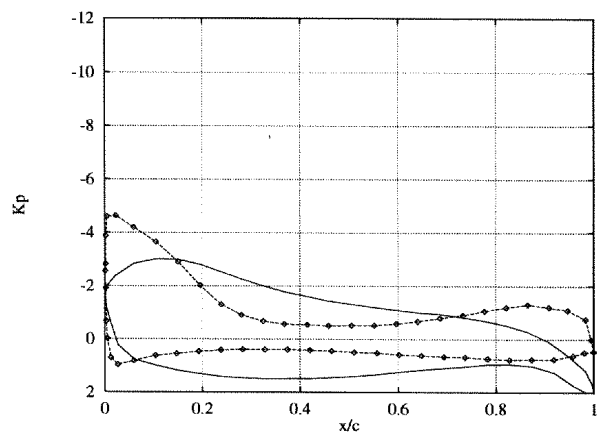


Figure 16. Shape #4 with inflated cells (Shape #5)

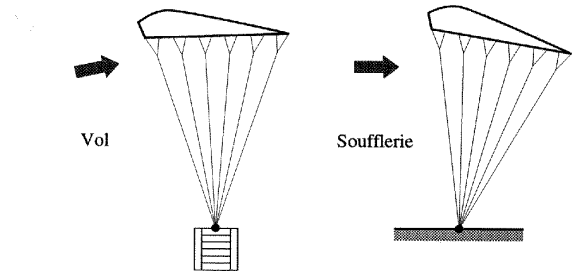


Figure 17. Comparison between flight and wind tunnel configurations

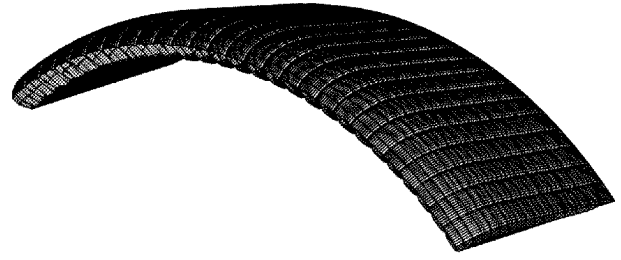


Figure 21. Deformed shell structure

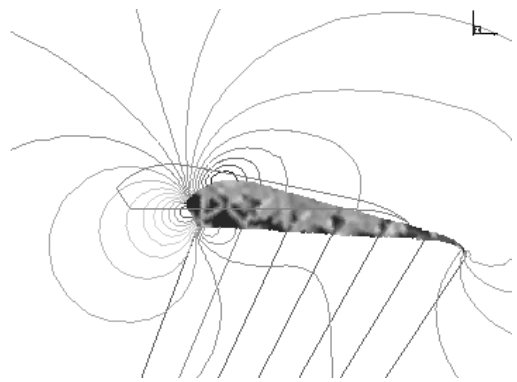


Figure 18. Equilibrium state computation

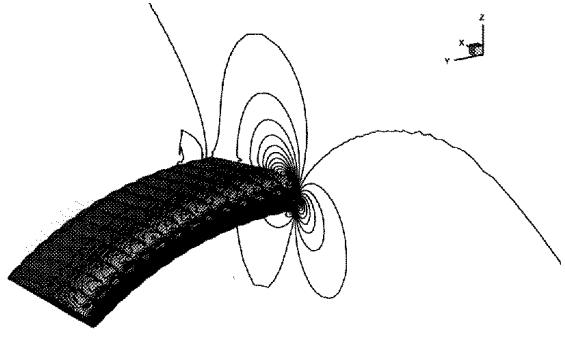


Figure 22. Aerodynamic computation on the deformed structure.

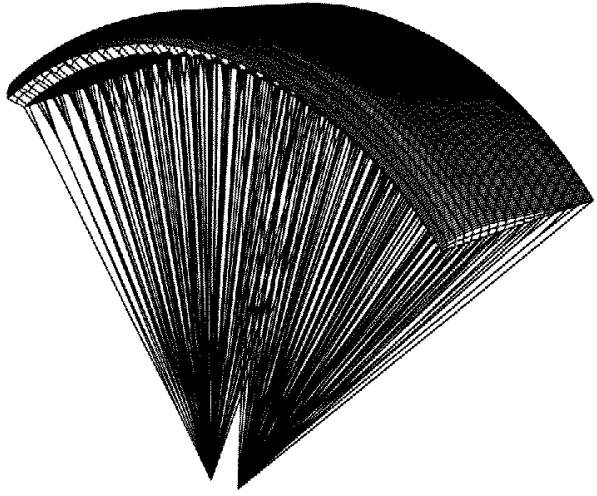


Figure 19. Undeformed structural model

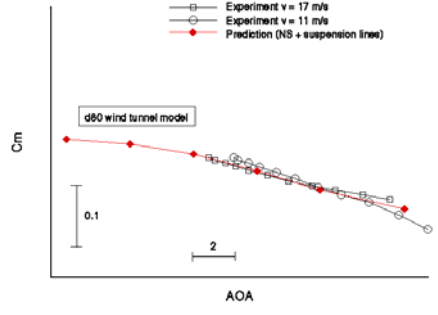


Figure 23 Pitching moment coefficient comparisons

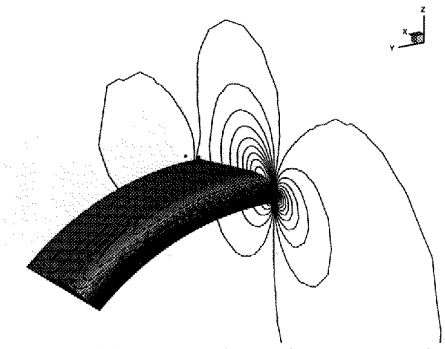


Figure 20. Aerodynamic computation on the reference shape

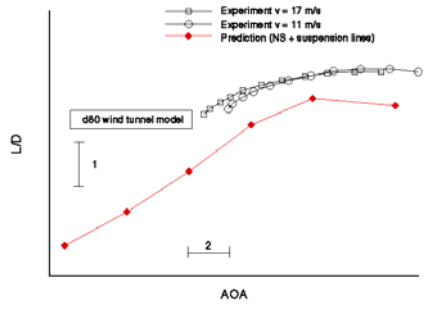


Figure 24 Lift-over-Drag ratio comparisons